Semicond. Sci. Technol. 4 (1989) 1061–1079. Printed in the UK

Interface trap transformation in radiation or hot-electron damaged MOS structures

T P Ma

Yale University, Centre for Microelectronic Materials and Structures, Department of Electrical Engineering, New Haven, CT 06520-2157, USA

Received in accepted form 23 August 1989

Abstract. The interface traps created by ionising radiation or hot-electron injection in MOS capacitors have been found to undergo significant changes with time over an extended period (many months). Immediately after radiation or hot-electron damage, an interface trap peak above the midgap ($\sim E_v + 0.75$ eV) invariably appears. This peak (designated peak 1), along with its background, would continuously change with time after damage, and the detailed time-dependent behaviour depends on the surface orientation of the Si substrate, processing history, gate bias and sample temperature. For samples made on (100) substrates, three separable regimes have been observed: (i) latent generation (peak 1 and its background increase with time), (ii) defect transformation (peak 1 gradually converts into peak 2 below the midgap, resulting in a double-peak interface trap distribution) and (iii) room-temperature annealing (the overall density of interface traps decreases with time). The focus of this paper is on the defect transformation process. For samples made on (111) samples, on the other hand, the most salient feature is the gradual shift of the energy position of peak 1 toward the valence band, and eventually a single peak residing below the midgap is observed. In contrast to the (100) results, no discernible double-peak distribution has been found in (111) samples. Results on (110) samples are qualitatively similar to those on (111) samples, while (311) samples are similar to (100) samples. The various experimental parameters that affect the defect transformation process in both (100) and (111) samples will be discussed. While the (100) results are too complex to be explained satisfactorily based on existing theories at the present time, the (111) results will be interpreted in terms of the atomic relaxation of the dangling-bond defect at the (111)Si/SiO_2 interface.

1. Introduction

Winokur *et al* were among the first to make a systematic observation of the post-irradiation behaviour of radiation-induced interface traps in MOS capacitors [1–3]. They reported that, under a positive gate bias (of order of 1 MV cm^{-1}), the interface trap density would continue to grow for a period of up to several hours at room temperature before it would saturate. On the other hand, under a negative gate bias, very little or no post-irradiation growth of the interface trap density was observed. It was found that the final value of the interface trap density depended on the radiation dose and the oxide field during irradiation, and the timescale for the post-irradiation build-up depended on the oxide field and the sample temperature after irradiation.

In those studies the focus was on the post-irradiation build-up of the overall density of interface traps, and not on their energy distributions.

Since the energy distribution of the interface traps may provide valuable information about the nature of the time-dependent evolution of these radiation-induced interfacial defects, we decided to make a more comprehensive study of their post-irradiation behaviour, with particular attention focused on any systematic changes of the energy distribution with time.

Initially, all our experiments were performed on samples fabricated on (100) Si substrates, not only because of their technological relevance, but also because of the availability of the samples. After extensive investigation on numerous samples, some fabricated at Yale and many others supplied by our industrial colleagues, we discovered that, although details did vary among the different samples, the time-dependent evolution of the post-irradiation interface traps in all the (100) samples showed qualitatively very similar behaviour. In general, a broad interface trap peak above the midgap ($\sim E_v + 0.75$ eV) appears right after irradiation. This characteristic peak (designated peak 1), along with its background, would continuously change with time after irradiation. Three different regimes have been identified: (i) latent generation (peak 1 and its background increase with time), (ii) defect transformation (peak 1 gradually converts into peak 2, a second peak below the midgap) and (iii) room-temperature annealing (the overall interface trap density decreases with time). Which of these three

0268-1242/89/121061+19 $02.50

regimes dominates depends on a number of parameters, including processing history, irradiation conditions, gate bias, gate-induced stress and sample temperature. By appropriately adjusting these parameters, it is possible to observe all three regimes in a given sample over a long period of time. Qualitatively similar time-dependent behaviour has been observed in samples where interface traps are generated by hot-electron injection.

Of the three regimes mentioned above, the interfacial defect transformation process in (100) samples, which results in a double-peak interface trap distribution, is the most interesting one, and is the focus of this paper.

Having found that the interfacial defect transformation process occurs generally in all the (100) samples studied, we were curious to know whether the same phenomenon would exist in samples of other orientations. In addition, some of our colleagues who have modelled the interfacial defects, notably Poindexter and Edwards [4], urged us to look into (111) samples on the grounds that the dangling-bond defect at the (111) interface is much simpler than its (100) counterpart, and therefore should be easier to understand. Consequently, we started a series of experiments using (111) samples; we also included some (110) and (311) samples for comparison.

In the (111) samples, we found that although a characteristic interface trap peak, very much like the peak 1 observed in (100) samples, also appears right after irradiation, its subsequent post-irradiation evolution is distinctly different. Apart from the latent generation and the annealing processes, which occur in both (100) and (111) samples under certain conditions, the most salient feature in (111) samples is the gradual shift of the energy position of the peak toward the valence band with time, and eventually a single peak residing in the lower half of the Si band gap is observed at the end of the interface trap transformation process; no discernible double-peak structure has been observed. The movement of the peak is a function of the gate-induced stress, the gate bias polarity and sample temperature. Because of its relatively simple defect configuration in theory, we have been able to explain qualitatively the (111) results based on the model calculations of Edwards [5].

The experimental details and some of the pertinent results are presented in the following sections.

2. Experimental details

The (100) Si MOS capacitor samples used in this study covered a wide range of gate electrode materials (e.g. Al, poly-Si, Mo, $TiSi_2$), various oxidation conditions (e.g. dry O_2, steam, with/without Cl, various oxidation temperatures) and processed at several different laboratories (Yale, GE, TI and Hitachi). Although the results to be presented here are for some specific sets of samples, qualitatively similar results have been observed in all the samples investigated. The (111), (110) and (311) MOS capacitors were fabricated at Yale University. The processing details are summarised below.

The Al-gate, dry oxide samples were fabricated at Yale on p-type (100), (111) or (311) Si, with the oxides grown at 1000 °C in dry O_2 followed by N_2 annealing for 30 min.

The Al-gate, wet oxide samples were grown pyrogenically on p-type (100) Si at Hitachi Central Research Laboratory. The oxidation temperature was 900 °C, and the subsequent N_2 anneal was done at the same temperature for 30 min.

The gate Al of both the dry and the wet oxide samples were deposited at Yale using a Ta boat evaporator. Post-metallisation annealing was done in forming gas at 450 °C for 30 min.

The Mo-gate samples were fabricated on n-type (100) Si at GE, with thermal oxides grown at 900 °C in $O_2 + 2\%$ trichloroethane (TCA) ambient, followed by an *in situ* post-oxidation annealing in N_2 for 30 min. The gate Mo was deposited by sputtering.

The poly-Si and the $TiSi_2$ samples were fabricated at TI, with the oxides grown in an $O_2 + 3\%$ HCl atmosphere at 950 °C, followed by *in situ* N_2 annealing. The poly-Si gate was deposited by low-pressure chemical vapour deposition to a thickness of 4500 Å, and the $TiSi_2$ gate was formed by sputtering 2000 Å of pure titanium on top of the poly-Si followed by reaction in a furnace at 675 °C in an $Ar + N_2$ atmosphere.

The irradiation source used was an x-ray beam generated from a W target bombarded by 40 keV electrons with a typical dose rate of 30 krads(Si)/min. A total dose of up to 24 Mrads(Si) was used for some of the samples. In most cases no gate bias was applied during irradiation, although in some cases a gate voltage of + 5 or − 5 V was applied to study the bombardment bias effects.

For hot-electron damage studies, constant-current Fowler–Nordheim injection was done using a HP 4145B semiconductor parameter analyser.

The interface trap distributions were analysed by measuring the high-frequency and quasistatic C–V curves, with a ramp rate of 0.01 V s^{-1}. Since it takes approximately 2–3 min to set the sample and to start the measurement, in this paper whenever we state that C–V curves are measured 'right after' irradiation we mean no additional delay beyond the 2–3 min mentioned above.

After x-ray irradiation and characterisation, the samples were stored at a constant temperature ranging from room temperature to 150 °C, and C–V measurements were made at several time intervals to monitor the time-dependent evolution of the generated interface traps. In most cases no gate bias was applied on the sample during storage; in some cases a gate bias of +5 or −5 V was applied to study the effects of the gate bias.

3. Results on (100) samples

3.1. Appearance of the double-peak interface trap distribution

Figure 1 shows the quasistatic C–V curves of a poly-Si gate MOS capacitor measured within three minutes after

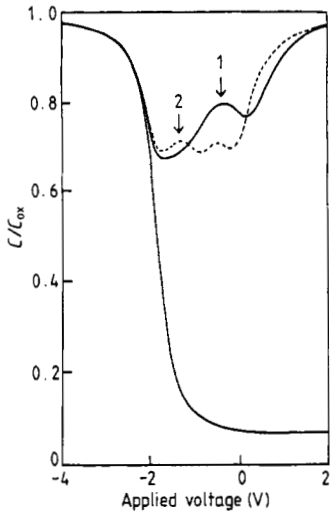

Figure 1. High-frequency and quasistatic C–V curves for a poly-Si gate MOS capacitor right after irradiation (full curve) and 2900 h later (broken curve). $A = 2.19 \times 10^{-3}$ cm^2; dose = 2 Mrad(Si); $d_{ox} = 250$ Å.

x-ray irradiation (full curve) and 2900 h after irradiation (broken curve). The sample was stored at room temperature with no bias on the gate between the two measurements. As one can see, shortly after irradiation only one peak was visible, corresponding to an interface trap peak in the upper half of the Si band gap ($\sim E_v + 0.75$ eV), which has been previously called the 'characteristic' peak in irradiated samples [6] and will be designated peak 1 in this paper. The sample was then stored at room temperature, and C–V measurements were taken at various intervals to examine its time dependence. Our results showed that peak 1 would decrease with time in this particular sample, and accompanying this was the formation and growth of a second peak in the lower half of the Si band gap (designated peak 2 hereafter). The broken curve in figure 1 exhibits clearly the appearance of the second peak after 2900 h of storage.

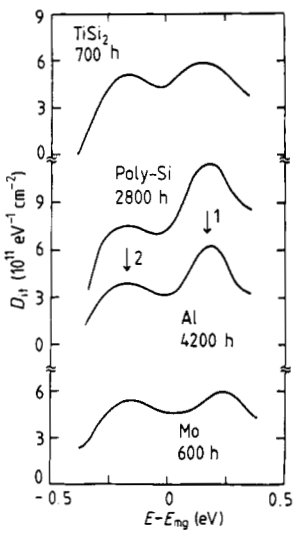

Figure 2. Interface trap distribution for four MOS capacitors with different gate electrodes, measured at various time intervals after the termination of x-ray irradiation. Only peak 1 appeared right after irradiation for all four samples. The oxide thickness is 500 Å for the Al-gate sample and 250 Å otherwise.

This second peak ($\sim E_v + 0.35$ eV) has been observed in a variety of samples made of different gate electrodes and with different oxidation conditions. Figure 2 shows the energy distribution of the interface trap density for four different MOS capacitors after x-ray irradiation and storage at room temperature for various lengths of time. For these capacitors no gate bias was applied during storage. Despite the fact that the gate electrodes are widely different, and the oxides were grown at different conditions, these samples all clearly show two peaks at late times after irradiation. In the case of the Al-gate sample shown here, peak 1 above the midgap continued to *increase* with time after irradiation for a long period of time (typically several months) until it started to saturate, and eventually showed a decreasing trend. During the period that peak 1 was increasing, there was no sign of peak 2. Only when peak 1 started to decrease did we observe the development of peak 2. For the other three samples, we only observed a *decrease* with time of peak 1 shortly after irradiation. Meanwhile, the development of peak 2 in these three samples appeared to occur over a shorter timescale. In fact, the general trend seemed to indicate that the growth of peak 2 is at the expense of peak 1, suggesting the possibility of the occurrence of some kind of interfacial defect transformation process, leading to a change in the energy distribution of the interface traps.

The interfacial defect transformation process will be discussed further in subsequent sections.

3.2. Time-dependent evolution of the interface traps

After analysing the data obtained on numerous samples produced in various laboratories, we found that the overall post-irradiation time-dependent behaviour of the interface traps may be characterised by three regimes: (i) latent generation (peak 1 and its background increase with time after irradition), (ii) defect transformation (peak 1 above the midgap gradually converts into peak 2 below the midgap) and (iii) annealing (the overall interface trap density decreases with time). One of the three dominates the observation at a given time, depending on several parameters, including the sample processing history, irradiation conditions, gate bias, sample temperature and time lapse after irradiation. One of the most influential parameters has been found to be the initial damage level (the interface trap density right after irradiation): for samples which had low initial damage, a latent generation process tends to dominate, at least in the initial phase, while room-temperature annealing tends to occur in highly damaged samples.

The latent generation process, we believe, corresponds to the same phenomenon reported by Winokur *et al* [1–3]. In agreement with their observation, we found that the latent generation process is enhanced with a positive gate bias while suppressed with a negative gate bias. On the other hand, we also observed latent genera-

tion in samples with no gate bias (gate floating) if their initial damage level was sufficiently low, although the rate of latent generation was lower than that with a positive gate bias.

In all cases, the interface defect transformation process, characterised by the gradual appearance and growth of peak 2, has generally been observed in (100) samples. For example, in samples that initially exhibit the latent generation process, peak 1 along with its background will increase for a period of time (up to several months in some cases) until it saturates. This is followed by a decreasing trend. When peak 1 starts to decrease, the defect transformation process becomes visible: the reduction of peak 1 is accompanied by the formation and growth of peak 2, until eventually a double-peak interface trap distribution is formed. For samples that have been heavily damaged, the defect transformation process is often accompanied by an overall reduction of the interface trap density (i.e. annealing) with time; especially at elevated temperatures.

The following section describes the interfacial defect transformation process in more detail.

3.3. Interfacial defect transformation process

3.3.1 Early evidence for interfacial defect transformation. The relationship between the growth of peak 2 and the reduction of peak 1 has been systematically studied in various (100) samples by monitoring continuously the time-dependent changes of both peaks. To calculate the net change of peak 2 as a function of time, we used a background subtraction procedure as described below.

Figures 3(*a*) and 3(*b*) show two examples of the interface trap distribution measured immediately after irradiation (dotted curve) and at later times (full curve) for two different MOS capacitors. Note that peak 2 appears very prominently on the full curve in either case, and it is riding on a background corresponding to the tail of the peak 1 distribution. Since evidence shows that this background is changing with time at the same rate as that of peak 1, we must subtract out this background effect to reveal more accurately the net change in peak 2. Using this procedure, we found that the amount of reduction in the magnitude of peak 1 corresponds almost exactly to the amount of growth in peak 2 for both samples exhibited in figures 3(*a*) and 3(*b*), providing additional support to the defect transformation idea.

More convincing evidence for the defect transformation model is presented below. Figures 4(*a*) and 4(*b*) show the time-dependent changes of peak 1 and peak 2, normalised with respect to the peak 1 value right after irradiation, for the two samples. If one follows the pair of peak 1 and peak 2 curves for either sample, one will notice that there is a strong correlation between the growth of peak 2 and the reduction of peak 1. In particular, note that the pair of curves for the Mo-gate sample (figure 4(*a*)) undergoes several up-and-down segments over the period of the experiment, and each up-going (down-going) segment in the peak 2 curve is correlated to a down-going (up-going) segment in the peak 1 curve. Moreover, the absolute changes in peak 2 are equal to those in peak 1 within experimental errors.

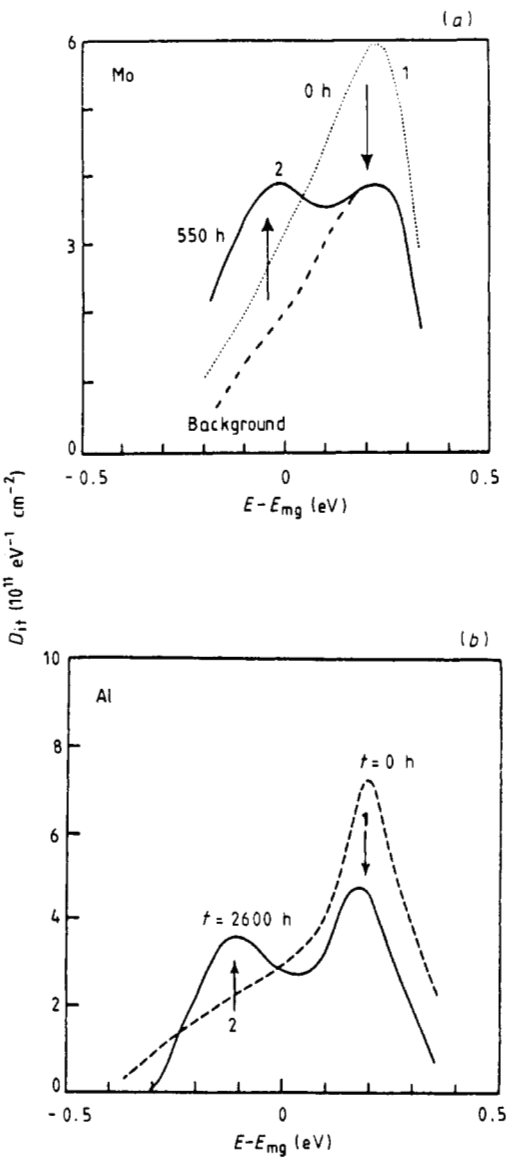

Figure 3. Interface trap distributions measured immediately after irradiation (dotted curve) and at later times (full curve) for two different MOS capacitors: (*a*) Mo-gate sample, 0.5 Mrad(Si) and (*b*) Al-gate sample, 2 Mrad(Si) (fluorinated)

One interesting feature of these results is the occurrence of a reverse transformation process (back-conversion of peak 2 into peak 1) in some cases when peak 2 has achieved a sufficient size, although the forward (peak 1 to peak 2) transition seems to be the dominant process over most of the period of the experiment. It is not clear what causes the reverse transformation in these samples.

Although we only showed here some results for x-ray irradiated samples, qualitatively similar results have been observed for hot-electron damaged samples as well (see § 3.3.4).

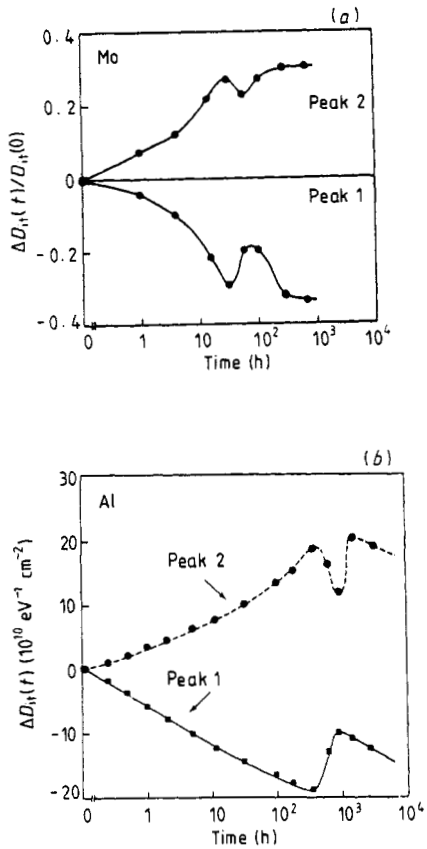

Figure 4. Time-dependent evolution of the magnitude of peak 1 (lower traces) and peak 2 (upper traces) for two different MOS capacitors after irradiation, showing strong correlation between the two peaks: (*a*) Mo-gate sample; (*b*) Al-gate sample (fluorinated). The magnitude of peak 2 has been obtained by the background subtraction method described in the text.

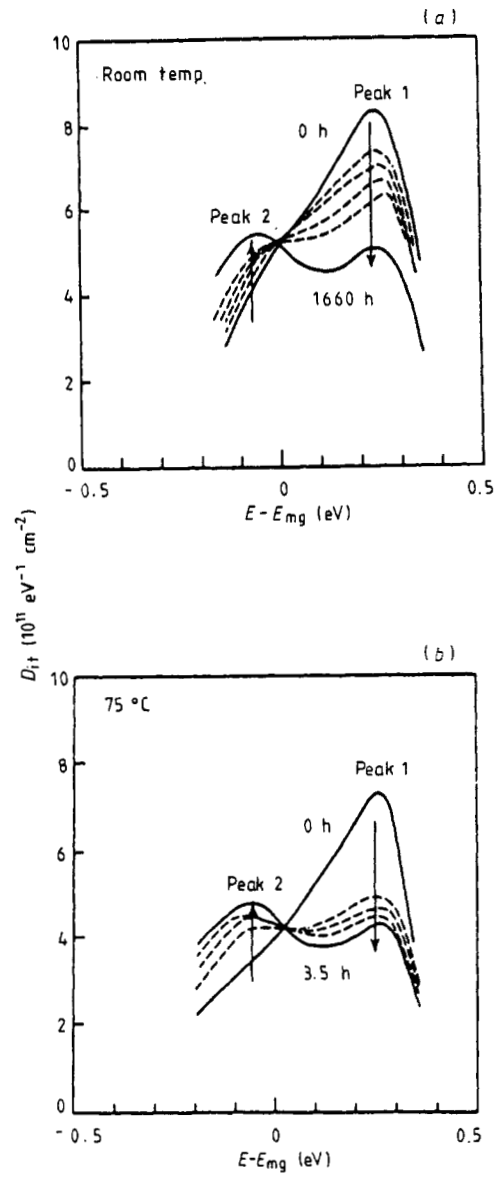

Figure 5. Interface trap distribution immediately after x-ray irradiation (curve marked 0 h) and some later times for Mo-gate samples: (*a*) stored at room temperature; (*b*) stored at 75 °C. The arrows indicate the directions of change in D_{it} with time. Note that the midgap density does not change with time. Dose = 2 Mrad(Si).

3.3.2. Interface traps at the midgap. One interesting feature we have observed is that, when defect transformation is the only process taking place at the interface (i.e. there is no annealing or latent generation), the interface trap density located at the midgap does not change with time even though other portions of the interface traps undergo drastic changes.

Some representative examples are shown below for a set of Mo-gate (dry oxide) samples (figure 5) and a set of Al-gate (wet oxide) samples (figure 6), with a storage temperature of room temperature (figures 5(*a*) and 6(*a*)) or 75 °C (figures 5(*b*) and 6(*b*)) after irradiation. It is apparent that in all cases the midgap interface trap density hardly changes throughout the entire defect transformation process. These examples are typical for devices in which only the defect transformation process occurs during the period of the measurements.

As mentioned previously, in addition to the defect transformation process some samples exhibit annealing or latent generation behaviour under certain conditions. In the case where the annealing process dominates, the midgap interface trap density has been found to decrease with time; while in the case where the latent generation dominates, we observe an increase of the midgap density with time. Thus the time dependence of the midgap density provides a convenient indicator for us to tell these three processes apart without having to analyse the interface trap spectrum throughout the band gap.

The fact that the midgap density does not change with time in (100) samples when only the defect transformation process is evident may arise from two possible sources. One possibility is that the energy width of the decreasing peak 1 extends beyond the midgap and into the lower half of the band gap, while the width of the increasing peak 2 also extends beyond the mid gap and into the upper half of the band gap. In this case, to obtain a midgap density that does not change with time, the rate of decrease of the peak 1 distribution at the midgap must be exactly equal to the rate of increase of the peak 2 distribution at the same energy position. Another possi-

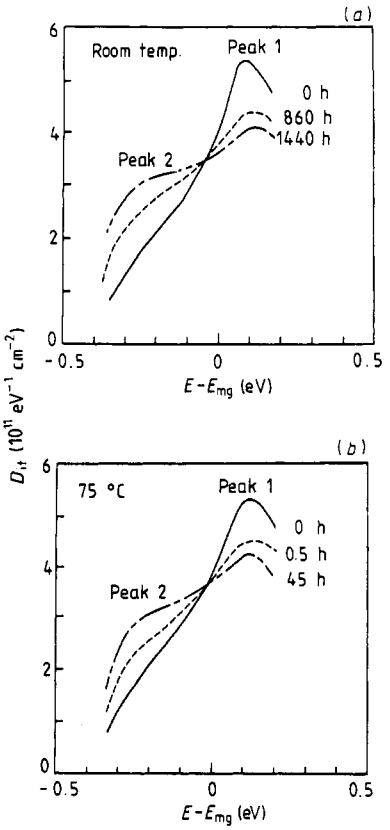

Figure 6. Interface trap distribution immediately after x-ray irradiation (curve marked 0 h) and some later times after irradiation in Al-gate (wet oxide) samples: (*a*) stored at room temperature; (*b*) stored at 75 °C. Note that the midgap density does not change with time. Dose = 0.3 Mrad(Si).

bility is that the transformation process resembles a seesaw motion with the midgap as the pivot, such that one side goes up while the other side goes down, with the pivot point staying motionless. We have not been able to determine from our experimental data which of the two is a more accurate description, although such information may help our eventual understanding of this process.

The next experiment provides strong evidence that peak 2 is not generated directly by ionising radiation, even after repeated x-ray irradiation, and a necessary condition for its formation is the pre-existence of peak 1.

3.3.3. Repeated damage-storage cycles. In this experiment, a set of Mo-gate MOS capacitors were first irradiated to a total dose of 2 Mrad(Si), followed by measurements of interface traps. These samples were then stored at 75 °C while their interface traps were monitored. Afterwards, the same experimental sequence, involving x-ray irradiation followed by periodic *C-V* measurements after storage at 75 °C, was repeated two more times on the same samples, and each time an x-ray dose of 2 Mrad(Si) was used. A post-irradiation sample storage temperature of 75 °C was selected to accelerate the transformation process (see § 3.3.5).

As shown in figure 7(*a*) only peak 1 appears immediately after the first x-ray irradiation (labelled 0 h), which decreases continuously while peak 2 begins to appear more and more prominently with time (see curves labelled 0.5 h and 23 h). Note that for this particular sample, in addition to the defect transformation process, thermal annealing is appreciable at 75 °C, as the midgap density decreases significantly with time.

After the first x-ray irradiation and storage at 75 °C for 23 h, at which time the interface trap distribution looked like the curve labelled 23 h in figure 7(*a*), the sample was again irradiated to a dose level of 2 Mrad(Si). As shown in figure 7(*b*), peak 1, along with its background, jumps back to a high level immediately after the second x-ray irradiation. In contrast, using the background subtraction procedure described earlier, we found that peak 2 did not increase at all as a result of the second x-ray irradiation.

After the second irradiation, the post-irradiation time-dependent behaviour of the interface traps has been found to be qualitatively similar to that after the first irradiation: continued reduction of peak 1 with a corresponding increase of peak 2 (see curves labelled 0.5 h and 21 h in figure 7(*b*)). The peak height of peak 2 after the second storage period, however, has become higher than that after the first irradiation-storage cycle.

The sample was then irradiated for the third time to a dose level of 2 Mrad(Si). This time the sample was stored and measured periodically for as long as 1000 h to investigate its longer-term time-dependent behaviour. As shown in figure 7(*c*), the time-dependent behaviour is again qualitatively similar to that in figures 7(*a*) and (*b*)

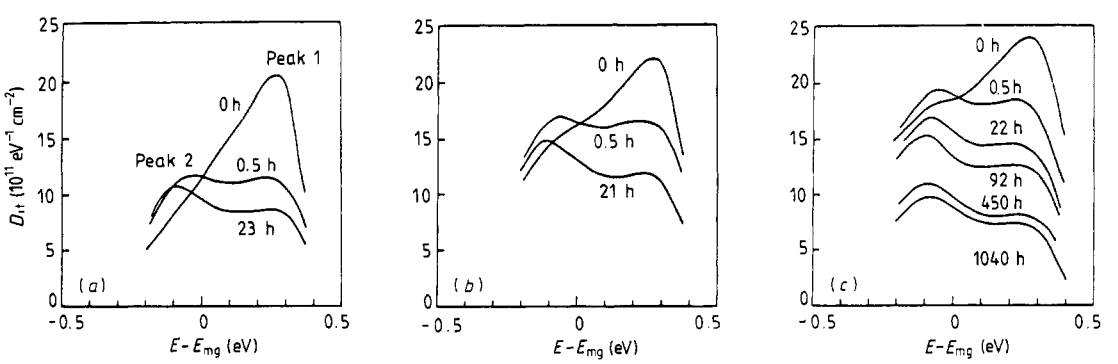

Figure 7. Interface trap distributions for a Mo-gate MOS capacitor measured immediately after irradiation (curve marked 0 h) and some later times after irradiation: (*a*) after first 2 Mrad(Si) irradiation and storage; (*b*) after second 2 Mrad(Si) irradiation and storage; (*c*) after third 2 Mrad(Si) irradiation and storage. The sample was stored at 75 °C between measurements.

up to 22 h of storage time. Thereafter, both peaks along with the background began to decrease at approximately the same rate, causing a downward parallel shift of the entire energy distribution (see curves below the one labelled 22 h in figure 7(*c*)), suggesting that thermal annealing becomes the dominant process.

The efffects of repeated irradiation-storage cycles are more clearly exhibited in figure 8, where the changes in the peak 1 height (lower curve) and the peak 2 heights (with background effect subtracted, upper curve) are plotted as a function of time after irradiation. The storage temperature was again 75 °C in all cases. It can be seen that, within each irradiation-storage cycle, there is a strong correlation between the growth of peak 2 and the reduction of peak 1 during the first hour; thereafter, peak 2 approaches saturation while peak 1 continues to decrease. Evidently peak 2 also decreases later after the apparent saturation level is reached due to annealing (see the peak 2 curve corresponding to the third irradiation-storage cycle).

The important point to note here is that peak 2 does not grow immediately after each x-ray irradiation, despite the fact that each time peak 1 shows a large increase. Instead, peak 2 only grows when peak 1 decreases, suggesting that the reduction of peak 1 is a necessary condition for the growth of peak 2. This is another strong piece of evidence in support of the defect transformation idea.

It should also be noted that, immediately after the second and third irradiations, peak 2 actually showed a slight decrease, suggesting the possibility of a reverse transformation triggered by the irradiation. Evidence for this reverse transformation phenomenon also exists in some other samples under different circumstances (see figures 4(*a*) and 4(*b*)), but its cause is not yet clear.

The saturation of peak 2 (which occurs after $\sim$ 1 h of storage at 75 °C for these samples) appears to indicate that a large portion, but not all, of peak 1 eventually converts to peak 2 at this temperature. The other fraction of peak 1 does not seem to undergo the defect transformation process described above (its reduction does not contribute to the growth of peak 2). After each repeated irradiation, however, more of the convertible peak 1 defect is again generated, and the peak 2 growth process proceeds accordingly.

3.3.4. Hot-electron-induced interface traps. All aspects of the time-dependent behaviour described above, including latent generation, defect transformation and annealing, have also been observed in samples damaged by Fowler-Nordheim hot-electron injection.

Figure 9 shows an example of the *C–V* curves for a poly-Si-gate MOS capacitor measured before (curve A), right after (curve B) and 32 h (curve C) after hot-electron injection. A broad peak in the quasistatic *C–V* curve (labelled 1) is clearly visible right after hot-electron injection. This peak is due to the same characteristic interface trap peak in the upper half of the Si band gap, peak 1, as that in radiation-damaged samples.

The post-injection evolution of the interface traps has been found to exhibit qualitatively similar behaviour to that of the radiation-induced interface traps. Curve C in figure 9 shows the development of a double-peak structure, suggesting that the interfacial defect transformation process also occurs in hot-electron damaged (100) samples.

Figure 10 is another example showing evidence of defect transformation in a hot-electron damaged MOS capacitor with an Al gate.

In both examples, the hot-electron injection was done with a positive gate bias so that electrons are injected

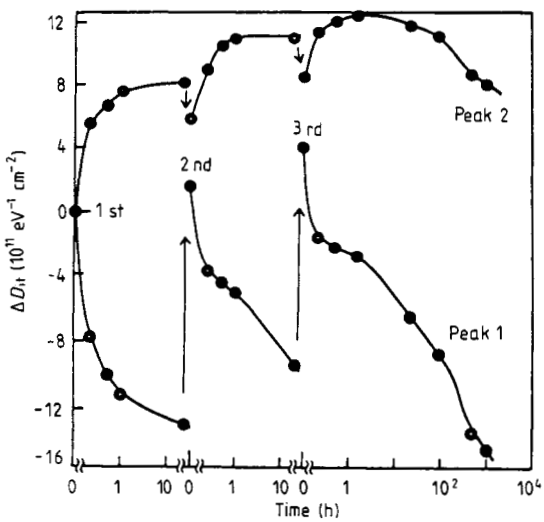

Figure 8. Time-dependent change of interface strap peak 1 above the midgap (lower curve) and peak 2 below the midgap (upper curve). The order in which irradiation was performed is marked. The sample was stored at 75 °C between measurements.

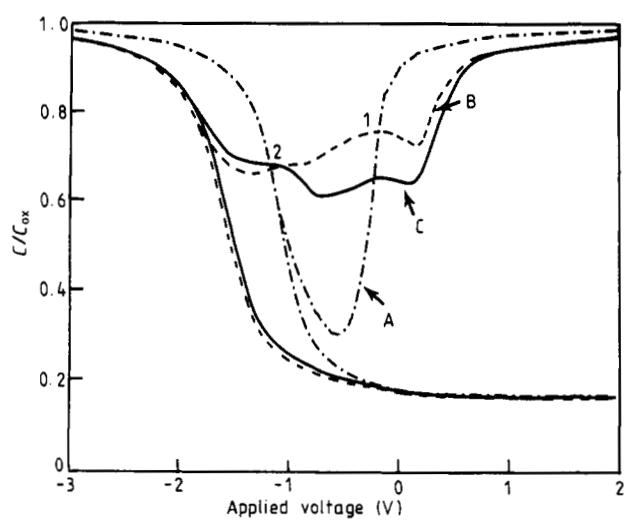

Figure 9. High-frequency and quasistatic *C–V* curves for a poly-Si-gate MOS capacitor before electron injection (A), right after electron injection (B), and 32 h after electron injection (C). The electrons are injected under a positive gate bias at a current density of 1.7×10^{-4} A cm^{-2}.

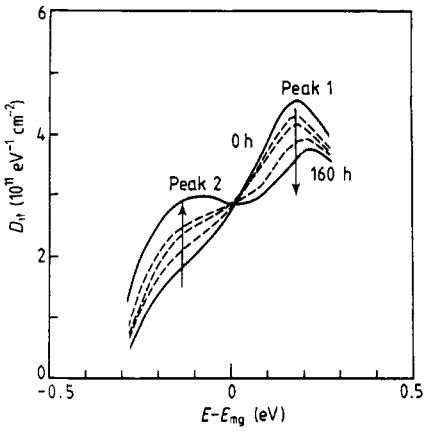

Figure 10. Interface trap distribution measured immediately after hot-electron injection (curve marked 0 h) and some later times for an Al-gate MOS capacitor. The electrons are injected under a positive gate bias at a current density of 5×10^{-5} A cm^{-2} for 200 s, at room temperature.

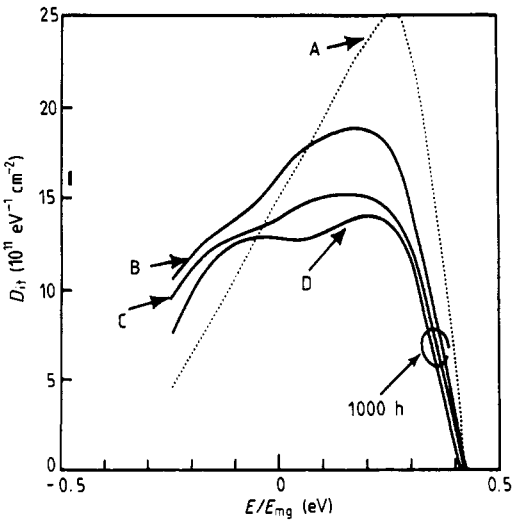

Figure 11. Interface trap distributions for three samples measured right after irradiation (curve A) and 1000 h after irradiation (full curves). The three samples were under different bombardment biases, and the total doses were adjusted to produce roughly the same density of interface traps for all samples: B, 24 Mrad(Si) and − 5 V; C, 1 Mrad(Si) and + 5 V; D, 2 Mrad(Si) and no bias.

from the Si substrate toward the gate electrode. It has been found that the time-dependent behaviour of the hot-electron-induced interface traps is strongly influenced by the gate voltage polarity during injection. This point will be discussed further in § 3.3.5.

3.3.5. Dependences of transformation on various parameters. As mentioned earlier, the interface defect transformation process depends on a variety of experimental parameters. Some of the more important parameters are summarised below.

Gate bias during irradiation. The effect of the gate bias during irradiation on the post-irradiation behaviour of the interface traps in (100) samples is illustrated in figure 11, in which the interface trap distributions for three MOS capacitors (which had three different gate biases during irradiation) are displayed.

The thin dotted curve roughly represents the distribution right after irradiation for all three samples. Since the radiation sensitivity depends strongly on the bombardment bias, we adjusted the radiation dose for each sample so that approximately the same density of interface traps was created. Thus, three different dose levels, 1, 2 and 24 Mrad(Si) were used for samples biased at + 5, 0 (floating) and − 5 V, respectively.

When measured 1000 h after irradiation, however, we found substantial differences among the three samples. It is apparent that the rate of reduction of peak 1 and its background is retarded with a gate bias of either polarity during irradiation, and a negative bombardment bias gives rise to the strongest retardation. After a more thorough investigation, we have concluded that there is a substantial room-temperature annealing component in addition to the defect transformation process in these samples, and the major difference among the three samples is the different annealing rates. The fact that the room-temperature annealing rates for the three samples are different is also evident in the data of figure 11, in which the midgap densities for the three samples follow the order B > C > D (see § 3.3.2 for a discussion of the midgap density during annealing).

Hot-electron injection polarity. As mentioned briefly in § 3.3.4, the time-dependent behaviour of hot-electron-induced interface traps depends strongly on the gate voltage polarity during injection.

Figure 12 compares the post-injection development of interface traps created by hot-electron injection under a positive gate bias during injection (figure 12(*a*)) and

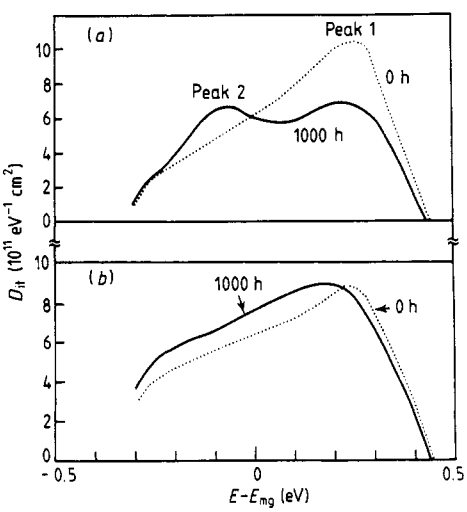

Figure 12. Interface trap distribution measured immediately after hot-electron injection and 1000 h after injection: (*a*) positive gate bias during injection; (*b*) negative gate bias during injection.

under a negative gate bias (figure 12(*b*)). Note that when measured 1000 h after injection, peak 2 is clearly visible in figure 12(*a*) but not in 12(*b*), indicating the strong influence of the injection polarity.

To find out whether the difference is due to the different origins of the hot electrons (the injected hot electrons originate from the Si substrate under a positive bias, while under a negative bias they originate from the gate electrode), or merely due to the different polarities of the oxide field, we investigated the bombardment-bias dependence of the same set of samples after irradition.

Figure 13 shows the results for a set of x-ray irradiated samples with a positive bombardment bias (figure 13(*a*)) and a negative bombardment bias (figure 13(*b*)). The magnitude of the bombardment bias was set to be sufficiently low so that it did not significantly affect the energies of the radiation-induced electrons and holes in the oxide. Again, it is apparent that the development of peak 2 is hindered in samples which had a negative gate voltage during irradiation.

The qualitative similarity between figures 12 and 13 leads us to believe that the difference between the results in figures 12(*a*) and 12(*b*) can be attributed to the polarity of the oxide field during hot-electron injection.

When the hot-electron-induced interface trap density is sufficiently low, we often observe a latent generation phenomenon in samples injected with a negative gate polarity as shown in figure 14(*a*), but not in samples injected with a positive gate polarity, as shown in figure 14(*b*). Note that no gate bias was applied on either sample after hot-electron injection. The effect of post-damage gate bias will be discussed below.

It should be noted that, while peak 1 in figure 14(*a*) continues to increase for a long time, its rate of increase will eventually reduce to zero, followed by a decreasing trend afterwards. The decrease in peak 1 is again accompanied by the formation and growth of peak 2.

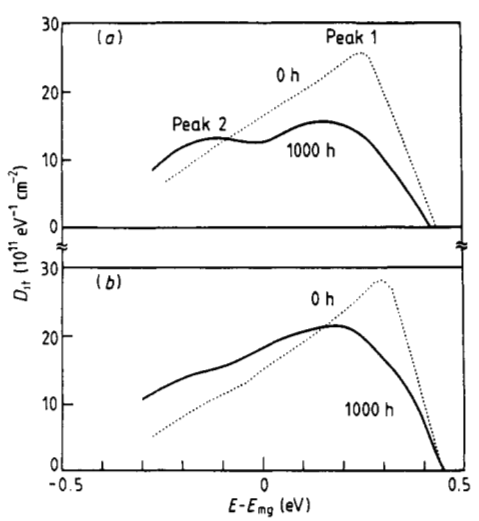

Figure 13. Interface trap distribution measured immediately after x-ray irradiation and 1000 h after irradiation: (*a*) 1 Mrad(Si), positive bombardment bias; (*b*) 24 Mrad(Si), negative bombardment bias.

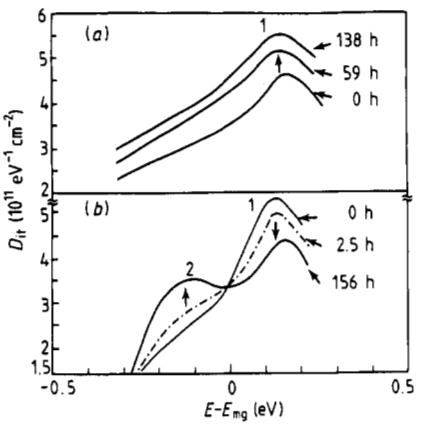

Figure 14. Interface trap distributions of Al-gate MOS capacitors at several time intervals after hot-electron injection at a current density of 6×10^{-6} A cm^{-2} for 200 s: (*a*) e^- injection from Al gate; $d_{ox} = 500$ Å; current density = 6×10^{-6} A cm^{-2}; time = 200 s. (*b*) e^- injection from substrate; $A = 3.2 \times 10^{-4}$ cm^2.

Gate-induced stress. It has been shown that the radiation sensitivity of a MOS capacitor depends systematically on the gate-induced stress [6]; in particular, the radiation-induced interface trap density has been found to be lower for a sample having a higher gate-induced compressive stress. Therefore, it is reasonable to suspect that the post-irradiation behaviour of the interface traps might also depend on the gate-induced stress.

Among other things, the gate-induced stress is a function of the thickness of the gate electrode material and the dimension of the gate electrode [6]. For example, for an Al-gate MOS capacitor, the thicker the Al electrode, or the smaller the gate-Al dimension, the larger the gate-induced compressive stress.

Figure 15 shows the post-irradiation change in the magnitude of peak 1 for a set of Al-gate MOS capacitors having three different Al thicknesses. In this particular set of samples, only a latent generation phenomenon is observed over the period of time of the experiment. It is

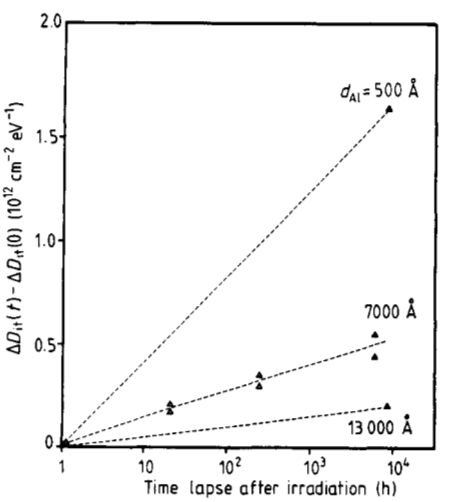

Figure 15. Post-irradiation time-dependent change of the magnitude of peak 1 for three Al-gate MOS capacitors with different gate-Al thicknesses. $d_{ox} = 500$ Å; 3 Mrad(Si).

apparent that the rate of latent generation is higher for a sample having lower gate-induced compressive stress.

Figure 16 shows the time dependence of peak 1 amplitude after hot-electron injection (under positive gate bias) for a set of (100) samples having three different gate dimensions. Two different injection current levels were used to create different degrees of damage. The injection period was 200 s for all samples. The dependence on gate size (thus the gate-induced stress) is evident for both sets of samples that received either a lower level of damage (curves A, B and C) or higher (curves D, E and F).

In addition to the gate size, the time-dependent behaviour is quite different between the two sets of samples that received different degrees of hot-electron damage. The dependence on the damage level will be further discussed below.

Sample storage temperature. All three components of the post-irradiation time-dependent behaviour, latent generation, defect transformation and annealing, have been found to be thermally accelerated.

Figures 17(*a*) and (*b*) show an example of the post-irradiation time-dependent evolution of peak 1 (lower half of each graph) and peak 2 (upper half) for a set of dry oxide (Mo-gate) and a set of wet oxide (Al-gate) samples stored at three different temperatures between measurements. In this case, defect transformation is the dominating process for both sets of samples at all three temperatures, as evidenced by the fact that the peak 2 curves are nearly the mirror image of the peak 1 curves.

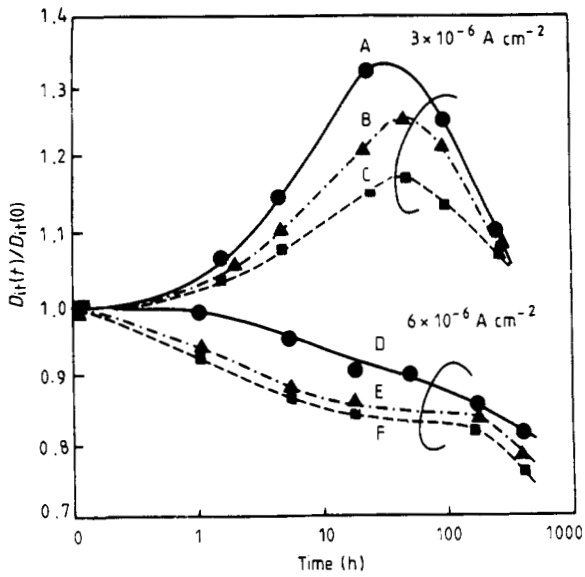

Figure 16. Time-dependent change of normalised peak 1 amplitude after electron injection (positive gate bias during injection) for a set of samples with three different gate-Al dimensions. The device areas are 4.1×10^{-3} cm^2 for curves A and D, 1.7×10^{-3} cm^2 for B and E, and 3.2×10^{-4} cm^2 for C and F. Two different injection current densities (as specified) are used for A–C and D–F, respectively.

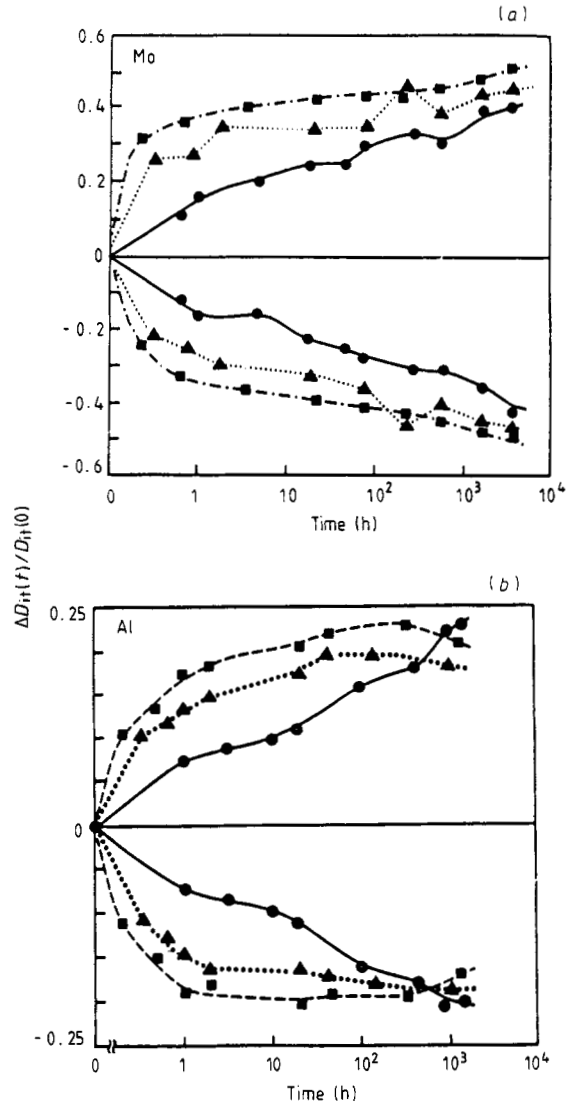

Figure 17. Time-dependent evolution of peak 1 (upper traces) and peak 2 (lower traces) for (*a*) Mo-gate samples (dry, TCA oxide) and (*b*) Al-gate samples (wet oxide) after irradiation and stored at three different temperatures; ●, room temperature; ▲, 50 °C; ■, 75 °C.

It should be noted that, although the rate of transformation is even higher at temperatures above 75 °C, we observed substantial annealing in the temeprature range 100–150 °C, and the annealing rate for peak 1 is higher than that for peak 2 at these elevated temperatures. As a result, given sufficient time, peak 1 will completely disappear, leaving a single peak (peak 2) distribution in the lower half of the Si band gap. This phenomenon is further discussed in § 3.3.6.

Sample storage bias. The dependence of the latent generation process on the gate bias after irradiation was first reported by Winokur *et al* [1-3]. This dependence has since been confirmed by researchers in several laboratories, including our own.

In addition, we have found that the interfacial defect transformation process also depends on the presence or absence of a gate bias and its polarity during storage.

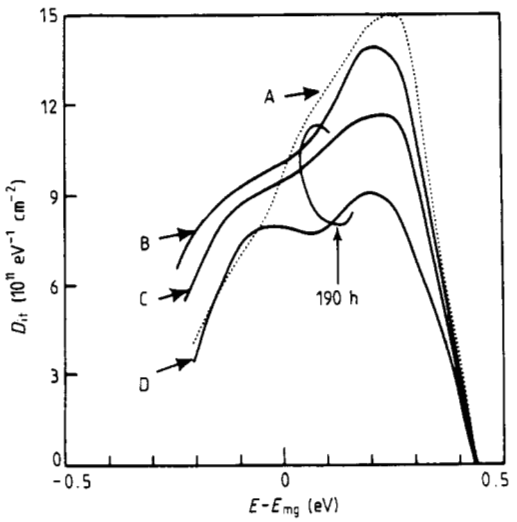

Figure 18. Interface trap distributions for Mo-gate MOS capacitors measured right after irradiation (curve A) and 190 h after irradiation (full curves). Dose = 0.5 Mrad(Si) and bombardment bias = + 5 V. The devices were stored at room temperature after irradiation with a gate bias of + 5 V (curve B), − 5 V (curve C) and no bias (curve D), respectively.

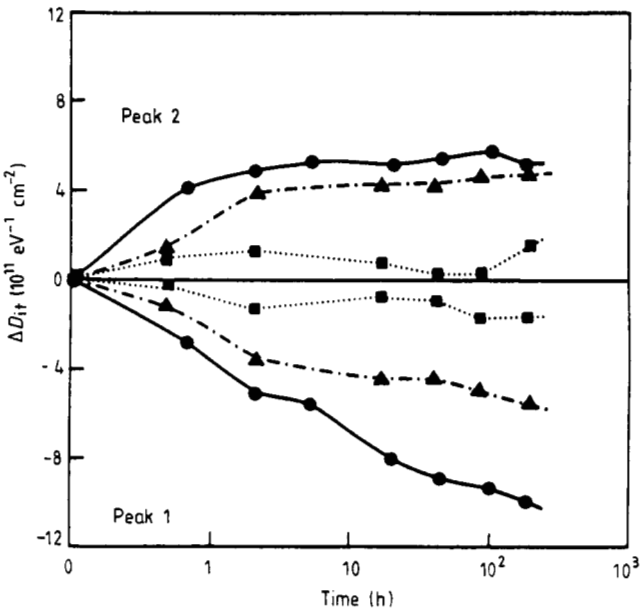

Figure 19. Time-dependent evolution of peak 1 and peak 2 for a set of Mo-gate MOS capacitors after irradiation and stored at room temperature under three different gate biases. Dose = 0.5 Mrad(Si); bombardment bias = + 5 V. Storage bias: ●, no bias; ▲, − 5 V; ■, + 5 V.

As shown in figure 18, the interface trap distributions right after irradiation (thin dotted curve) and 190 h after irradiation (full curves) are plotted. After irradiation, the samples were stored at room temperature with three different gate biases (+ 5 V and − 5 V, and gate floating) applied to three different samples. Notice that all three samples show a reduction of peak 1 when measured 190 h after irradiation, and the sample with no bias during storage exhibits the highest rate of reduction, with a correspondingly higher rate of growth in peak 2 (after background subtraction). The presence of a gate bias of either polarity during storage tends to retard the time rate of change, with positive bias giving rise to the strongest retarding effect.

Figure 19 shows the time dependence of the two peaks for the samples in figure 18 in more detail. Here the retarding effect of the gate bias, especially that of the positive gate bias, is evident throughout the entire period of the experiment. It should be noted that substantial reverse transformation (back-conversion of peak 2 into peak 1) occurs for a long period of time for the sample with a positive gate bias.

Note also that in this example appreciable room-temperature annealing has occurred in the sample with no gate bias, for peak 1 continues to decrease long after peak 2 has stopped growing

Initial damage level. Although many parameters influence the time-dependent behaviour of radiation/hot-electron-induced interface traps, one key parameter that determines the occurrence of latent generation, defect transformation, or room-temperature annealing has been found to be the initial damage level (the interface trap density measured right after damage) in a given device. When the initial damage level is low, the latent generation phenomenon is likely to occur, especially under a positive gate bias; when the initial damage level is high, room-temperature annealing is often observed.

Figures 20 and 21 show the initial damage level (in terms of the peak 1 amplitude) for a set of dry oxide (Mo-gate) samples as a function of the radiation dose and the injection current density, respectively. The regions where defect transformation, annealing or latent generation process occur are marked on the two figures. Note that there is a strong similarity between the two damaging processes, and that the initial damage level plays an important role in both.

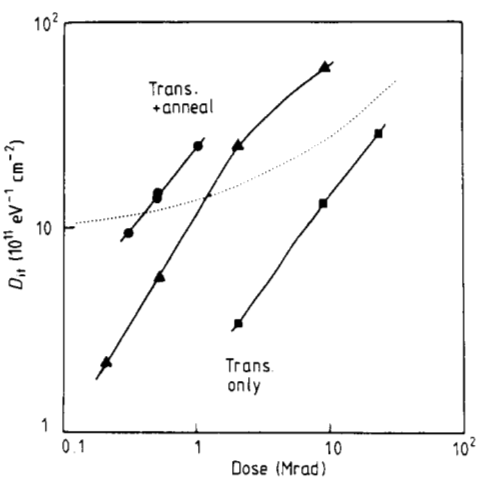

Figure 20. Magnitude of peak 1 measured right after x-ray irradiation as a function of x-ray dose for a set of Mo-gate MOS capacitors. The dotted boundary separates the regions where different time-dependent behaviour is observed. Bombardment bias: ●, + 5 V; ▲, no bias; ■, − 5 V.

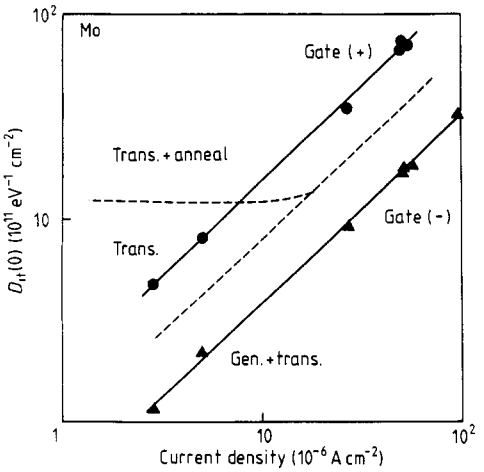

Figure 21. Magnitude of peak 1 measured right after electron injection as a function of injection current density (fluence). The dashed boundary separates the regions where different time-dependent behaviour is observed.

The similarity between the two damaging processes and the importance of the initial damage level in determining the time-dependent behaviour are shown even more convincingly in figure 22, where the changes in the peak 1 magnitude measured at several time intervals after irradiation or Fowler-Nordheim (F-N) electron injection are plotted on the same graph as a function of the initial damage level. The fact that both sets of data nearly fall on top of each other suggests that the initial damage level indeed governs the subsequent time-dependent behaviour of the interface traps, regardless of whether the damage was done by x-rays or hot electrons.

Another experiment which demonstrates the significance of the initial damage level is presented below. In this experiment (100) Si-gate MOS capacitors were used where the gate oxides were grown in dry O_2 containing 0-4% of TCA, and the effect of TCA concentration was studied.

Figure 23 shows that the magnitude of peak 1 measured right after irradiation increases monotonically with

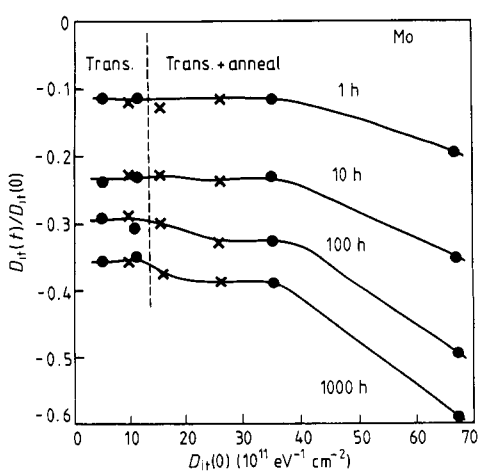

Figure 22. Relative changes in the magnitude of peak 1 measured at several time intervals after damage as a function of its initial value right after irradiation or hot-electron injection. ●, F-N injection; X, x-ray.

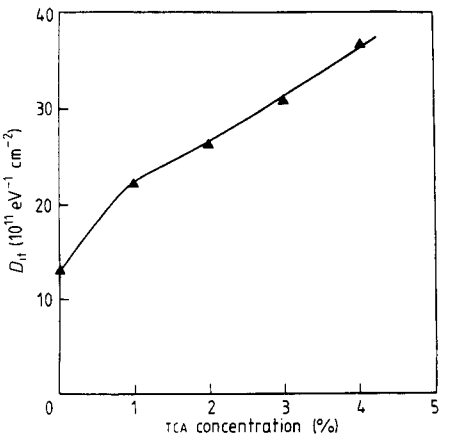

Figure 23. Magnitude of radiation-induced peak 1 as a function of TCA concentration for a set of poly-Si-gate MOS capacitors directly after x-ray. Dose = 1 Mrad(Si); d_{ox} = 250 Å; $A = 2.15 \times 10^{-3}$ cm^2.

TCA concentration. Actually, a minimum has been observed for TCA concentrations in the range 2-3 orders lower than 1% [7]. However, this is not relevant to the present discussion and will be neglected throughout the rest of this section.

Figure 24 shows the long-term time-dependent evolution of peak 1 and peak 2 for four samples with different TCA concentrations. Apparently there is a significant dependence on the TCA concentration. In particular, if one follows the set of peak 1 curves, one sees a latent generation phenomenon in samples with low TCA concentrations (0 and 1%) during the initial period, but not in samples with high TCA concentrations. Based on these data alone, one might easily conclude that the post-irradiation evolution of interface traps is a strong function of the TCA concentration incorporated during oxidation.

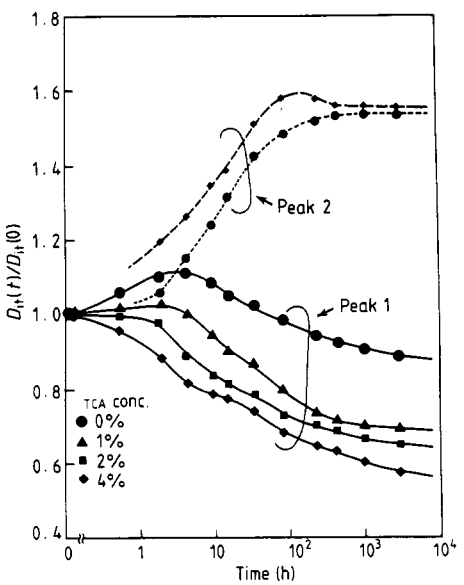

Figure 24. Post-irradiation time-dependent evolution of peak 1 and peak 2 for a set of samples oxidised with various TCA concentrations. Dose = 1 Mrad(Si); $A = 2.15 \times 10^{-3}$ cm^2; d_{ox} = 250 Å.

The reason that we did not jump to that conclusion was that the four samples in figure 24 above had significantly different initial damage levels (see figure 23), which might contribute to a good part of the observed apparent TCA concentration dependence. To examine the effect of the initial damage level, we used several different x-ray doses (0.5–4.0 Mrad(Si)) on each set of samples to create a wide range of initial damage levels, and subsequently analysed the changes in the magnitude of peak 1 for all samples as a function of the peak 1 value measured right after irradiation.

Figure 25 shows the results for these samples measured at four different times after irradiation. It can be seen that, despite the wide range of TCA concentrations, all data points lie on a straight line at a given time, and this trend is followed over a long span (three decades) in time. We thus conclude that the real controlling parameter in these samples is the initial damage level, not the TCA concentration, and the apparent TCA dependence shown in figure 23 is a result of the different initial damage levels produced by the x-ray irradiation.

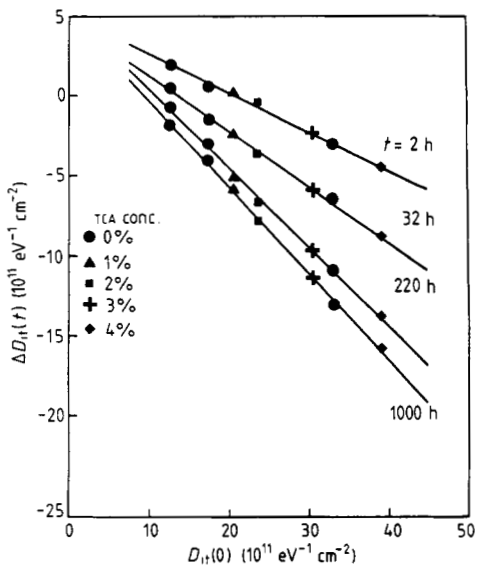

Figure 25. Changes in the magnitude of peak 1 measured at several time intervals after irradiation as a function of its initial value. Data include samples grown with various TCA concentration as specified. X-ray doses vary from 0.5 to 4 Mrad(Si).

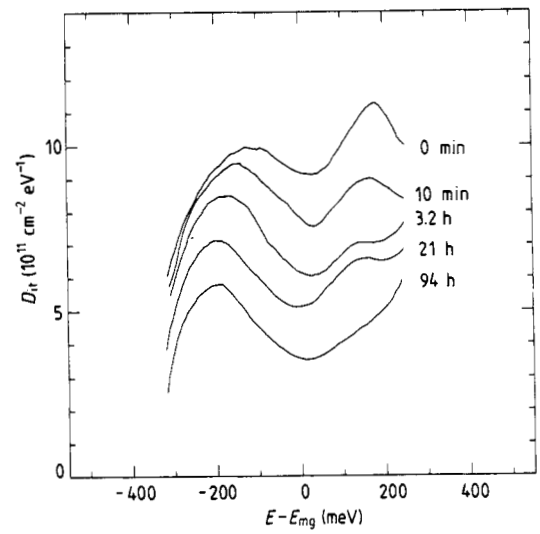

Figure 26. Post-irradiation interface trap distribution for an Al-gate (100) MOS capacitor after defect transformation process at room temperature, followed by annealing at 100 °C (times indicated on curves). Note that peak 1 gradually disappears at this elevated temperature. Dose = 1 Mrad(Si).

3.3.6. Disappearance of peak 1 at elevated temperatures. We have shown in the previous section that the interfacial defect transformation process may be accelerated by raising the temperature. When the temperature is too high, however, substantial thermal annealing of the interface traps may take place. In samples that have undergone defect transformation and exhibit a prominent double-peak interface trap distribution, we found that in the temperature range 100–150 °C the annealing rate of peak 1 can be substantially higher than that of peak 2 such that complete disappearance of peak 1 can be observed, leaving behind a single peak (peak 2) in the lower half of the Si band gap.

Figure 26 shows an example of this phenomenon for an x-ray irradiated Al-gate (100) sample. This sample was allowed to undergo the usual defect transformation process for three months at room temperature until both peak 1 and peak 2 became very pronounced. Then the sample temperature was raised to 100 °C to investigate the annealing effect. As shown in figure 26, at 100 °C the reduction of peak 1 is faster than that of peak 2, and after three days at 100 °C peak 1 becomes invisible. A similar effect has also been observed at 150 °C, except that the annealing rate is higher than at 100 °C.

These results, combined with those related to the defect transformation, suggest strongly that peak 2 is a more stable defect configuration than peak 1. This will be discussed further in § 6.

4. Results on (111) samples

The results presented so far have all been obtained on MOS capacitors fabricated on a (100) Si substrate. While they are very interesting, the results are too complicated to be explained satisfactorily using existing theories. Following suggestions made by some of our knowledgeable colleagues, notably Poindexter and Edwards [4], we decided to investigate (111) samples. The rationale is that the dangling-bond defect configuration at the (111)Si/SiO_2 interface is a lot simpler than that at the (100)Si/SiO_2 interface, at least in theory [5, 8]. Therefore, one may have a better chance of understanding the (111) results, which will in turn shed new light on the (100) problem.

This section presents the results of our recent study on the post-irradiation behaviour of the interface trap

distribution in MOS capacitors made on (111) Si substrates. It will be shown that the interface trap distribution in these (111) samples measured right after x-ray irradiation is qualitatively similar to what was observed in the (100) counterpart: a prominent peak appears in the upper half of the Si band gap. As far as we can tell, there is no appreciable difference between this peak and the peak 1 found in (100) samples.

The subsequent time-dependent evolution behaviour of this peak, however, is distinctly different for samples with the two different orientations. While in (100) samples the defect transformation process is characterised by the gradual conversion of peak 1 into peak 2 below the midgap, resulting in a double-peak interface trap distribution, the most salient feature observed in (111) samples is the gradual shift of the peak position with time toward the lower half of the Si band gap, and eventually a single peak will reside below the midgap. The movement of this peak has been found to be thermally accelerated, with an apparent activation energy of about 0.4 ± 0.1 eV. It has also been found that the gate-induced compressive strain at the Si/SiO_2 interface plays an important role in the peak movement. In addition, the presence of a gate bias and its polarity also significantly affect the post-irradiation behaviour of the interface trap distribution.

Figure 27 shows an example of the interface trap distribution in a (111) MOS capacitor measured right after irradiation (curve labelled 0 min) and at several later times. While a post-irradiation storage temperature of 80 °C was used in this example to accelerate the process, qualitatively similar behaviour has been observed at room temperature, except that a longer timescale is involved. Note that when measured right after irradiation the interface trap distribution resembles that found in (100) samples: a broad peak appears above the midgap, similar to the characteristic peak designated peak 1 in (100) samples. However, unlike the results for (100) samples, subsequent measurements on (111) samples show no indication of the development of a double-peak distribution. Instead, the most notable time-dependent behaviour is the gradual shift of the peak position with time toward the lower half of the Si band gap, and eventually the peak will reside below the midgap. There is also a continuous reduction of the interface trap density throughout the accessible energy range, characteristic of thermal annealing. Qualitatively similar results have been obtained on several different sets of samples made on (111) Si substrates obtained from two different suppliers.

The shift of the peak position with time is thermally accelerated, as shown in figure 28 where the peak position as a function of time is plotted for three different storage temperatures. Each data point is the average of at least three measurements, and the error bar of about 15 meV is the worst case standard deviation resulting from the determination of the peak position using the C-V measurement. The full curves are results of non-linear regression fitting to a simple exponential function $E_p = A \times \exp(-t/\tau) + B$, where E_p is the peak position in the Si band gap and τ is a temperature-dependent characteristic time constant associated with this peak movement. Note that data are shown here only after the peak has moved below the midgap; the movement of the peak in the upper half of the band gap is too fast (especially for storage temperatures above room temperature) to be accurately determined by our experimental technique.

We have calculated the time constants for several different storage temperatures, and found that they follow the Arrhenius relation: $1/\tau = 1/\tau_0 \times \exp(-E_a/kT)$, with an apparent activation energy E_a of about 0.4 ± 0.1 eV (see figure 29).

The post-irradiation behaviour of the interface traps is substantially different if a gate voltage of either polarity is applied during storage. Figure 30 shows the post-

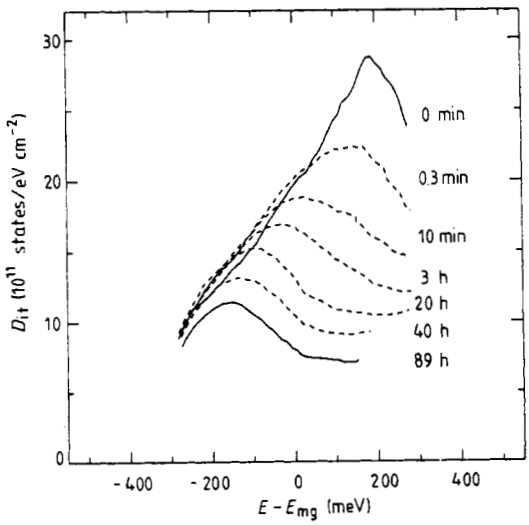

Figure 27. Interface trap distribution for a (111) MOS capacitor measured immediately after irradiation (curve labelled 0 min) and at several later times. A post-irradiation storage temperature of 80 °C is used in this experiment to accelerate the process. Dose = 0.5 Mrad(Si).

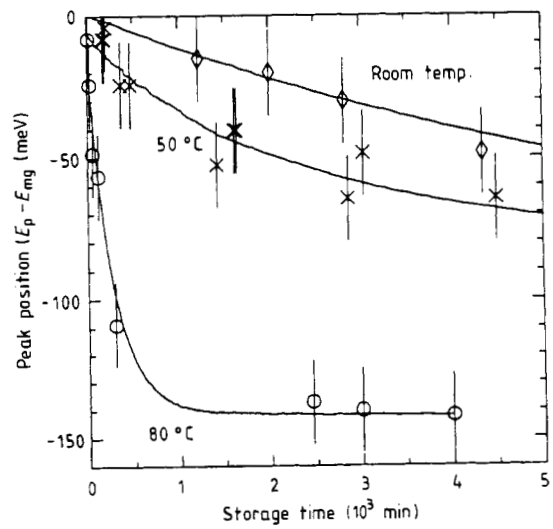

Figure 28. Post-irradiation interface trap peak position as a function of time at three different storage temperatures for a set of (111) MOS capacitors. Full curves are results of fitting to $A \exp(-t/\tau) + B$.

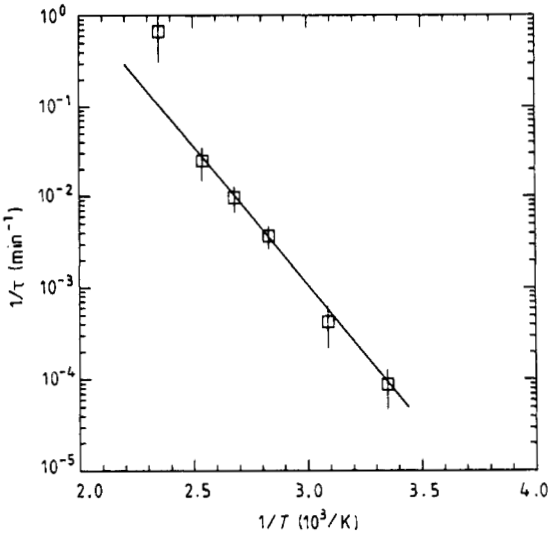

Figure 29. Arrhenius plot of the inverse time constant, $1/\tau$. The apparent activation energy E_a is about 0.4 ± 0.1 eV.

irradiation evolution of the interface traps at 50 °C, with a gate voltage of − 5 V (figure 30(*a*)) and + 5 V (figure 30(*b*)) applied. In the case of the negative gate bias (figure 30(*a*)), the dominant process seems to be an overall reduction (annealing) of the interface traps throughout the energy band gap, and a gradual broadening of the distribution. During the early stages of the development when the peak is still visible, it appears that the energy shift of the peak position is retarded by the negative gate bias. In contrast, in the case of the positive gate bias (figure 30(*b*)) the peak is clearly discernible throughout the period of the experiment, with a much more rapid shift of its energy position. In addition, the annealing process is greatly suppressed, resulting in a peak below the midgap whose density is not too much below the value when the peak is above the midgap.

To investigate the effect of the gate-induced interfacial stress on the post-irradiation behaviour of the interface traps, we performed an experiment on a set of samples that did not receive post-metal-anneal (PMA) treatment. It has been shown that for an Al-gate MOS capacitor the gate-induced stress is very small without PMA, while PMA causes a significant increase of the gate-induced compressive stress [6].

The result obtained on this set of non-PMA samples is represented by the data shown in figure 31. In contrast to the results shown in figure 27, there is no significant peak movement toward the valence band in this non-PMA sample (note the much longer timescale used in figure 31), and there is a substantial broadening of the distribution. This trend is not significantly affected by either a positive or a negative gate bias during storage.

As a summary, we have shown that the post-irradiation behaviour of the interface traps in MOS capacitors made on (111) Si substrates can be characterised by a gradual shift of the peak position toward the lower half of the Si band gap. The movement of the peak position is affected by the local environment of the interfacial bonding defects, including the gate-induced strain, the charge

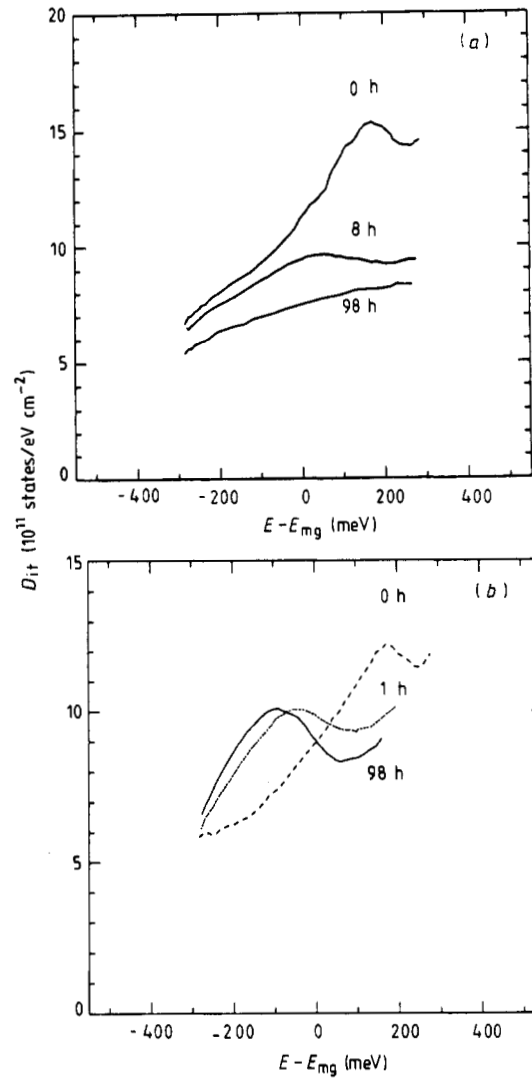

Figure 30. Post-irradiation interface trap evolution for samples stored at 50 °C, with a gate bias of (*a*) − 5 V or (*b*) + 5 V applied during storage (times after x-ray indicated on curves). Dose = 0.5 Mrad(Si).

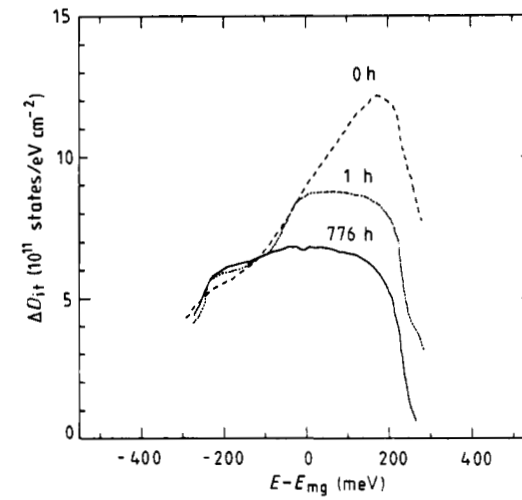

Figure 31. Post-irradiation interface trap evolution for a device that receives no PMA treatment prior to irradiation. The device is stored at 50 °C with gate floating. All curves are obtained by subtraction of the pre-irradiation curve. Dose = 0.15 Mrad(Si).

state of the defects (as affected by the gate bias polarity), and sample temperature. Compared to their (100) counterparts, the post-irradiation behaviour of the interface traps in (111) samples appears to be much less complicated, and there is a strong possibility that a reasonable understanding of the (111) results may be achieved based on existing theories (see §6).

5. Results on (110) and (311) samples

Encouraged by the (111) results, we decided to investigate samples of other orientations. We were particularly interested in the (110) samples, because it has been shown theoretically that the local environment of the dangling-bond defect at the (110)Si/SiO_2 interface is very similar to that at the (111)Si/SiO_2 interface [9], which is also in agreement with spin resonance data [11].

It should be mentioned that the samples of (111), (110) and (311) orientations reported in this paper were all cut from the same Si ingot, and processed the same way at Yale University. Therefore, we believe the differences in the experimental results can be attributed to the differences in the wafer orientation.

As it turned out, apart from some differences in the details, the (110) samples did indeed exhibit qualitatively similar behaviour to the (111) samples, and the (311) samples behaved in a manner very much like that of the (100) samples.

Figure 32 shows the post-irradiation evolution of a (110) sample at a temperature of 50 °C. As in samples of other orientations, a broad peak above the midgap appears right after irradiation. Compared to those in (100) and (111) samples, however, this peak in the (110) sample is significantly broader. When measured at some later times after irradiation, we observed a gradual shift of the energy position of the peak toward the valence band, much as we saw in (111) samples.

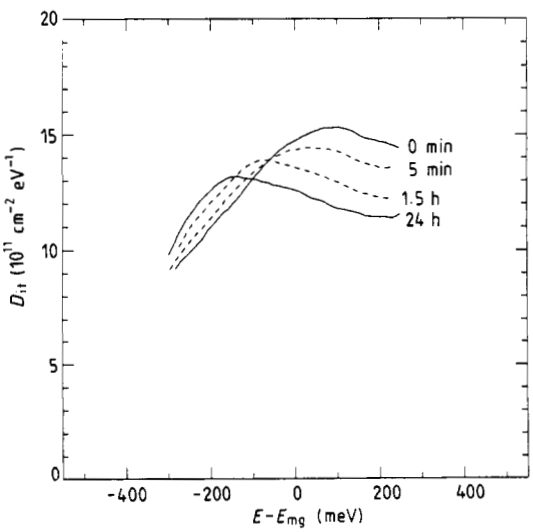

Figure 32. Post-irradiation evolution of interface trap distribution in (110) sample, showing the shift of the peak position toward valence band. Storage temperature = 50 °C, dose = 0.5 Mrad(Si).

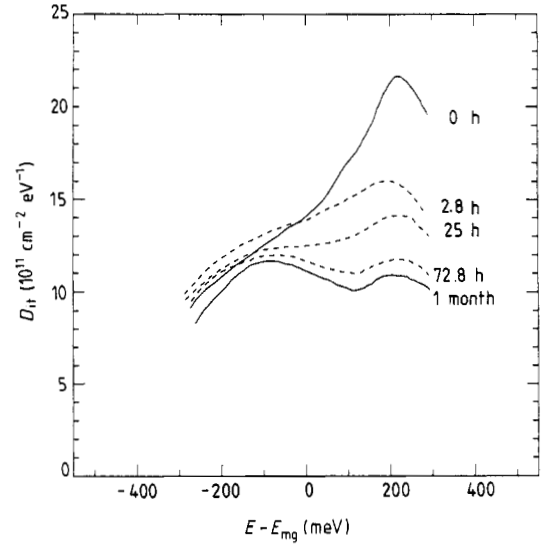

Figure 33. Post-irradiation evolution of interface trap distribution in (311) sample, showing the development of double-peak structure. Storage temperature = 50 °C, dose = 0.5 Mrad(Si).

Figure 33 shows the results for a (311) sample, where the peak right after irradiation appears to be sharper than those in any other orientation. The subsequent evolution of the interface trap distribution at 50 °C seems to be comparable to that in (100) samples, and a double-peak structure becomes visible when measured 30 min after irradiation. The peaks appear to be shallower than those in (100) samples.

No experiments have yet been performed on these samples to investigate the effects of gate bias, gate-induced stress and temperature.

6. Summary and discussion

The radiation-induced interface traps in Si MOS capacitors have been found to undergo continuous changes at room temperature for a long period of time after they are generated. After extensive measurements on a wide range of samples, we have observed the following general pattern: right after irradiation (as defined in § 2), a prominent characteristic interface trap peak above the midgap (designated peak 1) appears, and its subsequent evolution as a function of time depends on the orientation of the Si substrate and several other experimental parameters. The results are qualitatively similar for interface traps generated by hot-electron injection.

For (100) samples, the post-irradiation time-dependent behaviour of the interface traps can be classified into three regimes: latent generation (peak 1 and its background increase with time after irradiation), defect transformation (peak 1 gradually converts into peak 2 below the midgap, resulting in a double-peak distribution), and room-temperature annealing (the overall density of interface traps decreases with time). While many parameters influence the overall behaviour, a key parameter that determines which of the three regimes dominates is the

initial damage level (the density of interface traps measured right after irradiation): the latent generation process tends to occur for low initial damage levels, while the annealing process tends to prevail for high initial damage levels. We observed the defect transformation phenomenon in all (100) samples that we studied. Even in samples that exhibit the latent generation phenomenon during the initial period (which could be as long as several months at room temperature), peak 1 will eventually turn around and start to decrease, and the defect transformation process will begin.

In the defect transformation regime of (100) samples, the interface trap density at the midgap does not change with time, even though other portions of the interface trap distribution undergo drastic changes. In the latent generation regime, the midgap density increases with time, while in the annealing regime it decreases with time. Therefore, the time-dependent behaviour of the midgap density provides a convenient indicator showing whether the sample is undergoing latent generation, defect transformation or annealing.

The rate of defect transformation depends on various parameters. Among those studied, the gate bias polarity during irradiation and transformation, and sample temperature cause the most significant effects. The presence of a gate bias of either polarity, during either irradiation or post-irradiation storage, tends to retard the defect transformation process in (100) samples. A positive gate bias during post-irradiation storage gives rise to the strongest retarding effect.

Our experimental evidence suggests that peak 2 below the midgap is not generated directly by irradiation. The pre-existence of peak 1 above the midgap seems to be a necessary condition for the subsequent formation of peak 2.

In the temperature range between room temperature and 75 °C, it appears that only a portion of the peak 1 defect will eventually convert into peak 2 in (100) samples, and after the completion of the defect transformation process a two-peak interface trap distribution remains.

After peak 2 has acquired sufficient magnitude in (100) samples, a reverse transformation (back-conversion of peak 2 into peak 1) could occur under certain conditions, particularly when a positive gate bias is applied.

When the post-irradiation temperature is held at 100 °C or higher, substantial thermal annealing takes place, and the annealing rate for peak 1 is higher than that for peak 2, so that eventually peak 1 may completely disappear, leaving behind a single peak below the midgap.

The energy distribution of the two-peak interface traps resembles very closely that of the as-oxidised (without post-oxidation and post-metallisation anneals) (100) Si MOS samples reported by Gerardi *et al* [8]. The interface traps in such as-oxidised samples have been correlated with P_b centres by the use of ESR measurements [8]. It is not clear whether the double-peak distribution we have observed in samples which underwent the defect transformation process corresponds to those seen in as-grown samples. Substantial evidence suggests that they are rather different. The two peaks associated with the P_b centre mentioned above supposedly arise from an amphoteric defect; i.e. both interface trap peaks come from the same defect but measured at different Fermi levels. Therefore, one expects to observe two peaks at all times as long as there is measurable number of P_b defects. In our case, however, only peak 1 is observed right after irradiation, and the double-peak interface trap distribution takes a long time to develop. In addition, the fact that the ratio between the two peaks changes continuously with time, and peak 1 can be preferentially annealed out at a temperature above 100 °C, is also hard to understand using the simple P_b concept. In any case, it would be interesting to investigate the ESR signals of the radiation-induced interface traps during the defect transformation process.

In contrast to the (100) results, the post-irradiation time-dependent behaviour of the interface traps in (111) samples is much simpler. Apart from thermal annealing, the main effect is a gradual shift of the radiation-induced interface trap peak toward the valence band, and eventually this peak will move into the lower half of the Si band gap; no double-peak structure has been observed.

The movement of the interface-trap peak in (111) samples is a strong function of the gate-induced stress, the post-irradiation gate bias polarity and sample temperature.

In Al-gate samples which did not receive a post-metal-anneal treatment, so that the gate-induced stress is small, the above-mentioned peak movement is substantially suppressed, and replaced by a broadening of the interface trap distribution.

The presence of a negative gate bias after irradiation retards the peak movement toward the valence band, while the presence of a positive gate bias tends to enhance the peak movement but slows down the annealing rate.

The peak movement is thermally accelerated. In the absence of a gate bias, an apparent activation energy of around 0.4 eV has been obtained.

While a lot more work remains to be done before we can achieve a real understanding, our (111) results so far seem to be consistent with the model calculation of Edwards [5], in which he showed that the energy level of the interfacial defect state at the (111)Si/SiO_2 interface depends on the atomic relaxation of the tetrahedral configuration of the bonding defect (see figure 34). More specifically, he showed that the defect state energy increases (decreases) as the defect atom moves closer to (further from) the plane containing its three nearest-neighbour silicon atoms, while the top of the valence band stays relatively constant. To shift the energy by a few tenths of an eV only requires an atomic movement of a few per cent of the lattice constant, which does not seem unreasonable for a broken-bond defect to relax over the timescale of our experiment. He also stated in the same paper that, under significant compressive strain, the defect energy level will move toward the valence band as the defect atom moves toward the oxide, which is the case for our PMA samples in which considerable gate-Al-

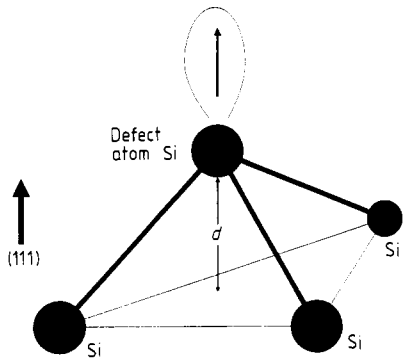

Figure 34. Schematic diagram showing Si tetrahedron containing a dangling-bond Si defect, where *d* is the distance between this defect atom and the plane containing its three nearest neighbours.

induced compressive strain exists at the interface [6]. This argument is also consistent with the observation on the non-PMA samples (see figure 31). It has been shown that for Al-gate devices that have not recieved a PMA treatment, the gate-induced interfacial strain is very small [6]. Without a large gate-induced compressive strain as a driving force, a defect atom would tend to stay at its initial position, causing no change in its energy level. This may explain the observed lack of peak movement in non-PMA samples.

According to Edwards [5], the charge state of the defect atom also plays an important role in the equilibrium configuration of the tetrahedron, and hence the energy levels of the defect. Positively charged defects tend toward a shorter *d* (see figure 34) than in the neutral state, while negatively charged defects tend toward a *slightly* longer one.

The charge state of a defect can be altered by applying an appropriate gate voltage. For a positive gate bias, most of the interfacial defects will be negatively charged, and one would expect the defect atom to seek an equilibrium configuration away from its three neighbouring Si atoms. This driving force is in the same direction as that due to the gate-induced stress, and the end result of the long-term positive bias is a longer *d* (see figure 34) than that without a gate bias. This is consistent with the fact that the energy position of the interface trap peak clearly shifts toward the valence band after long-term positive gate bias stress, as shown in figure 30(*b*). On the other hand, under a negative gate bias, most of the interfacial defects will be positively charged, giving rise to a tendency for the defect atom to move closer to its three neighbouring Si atoms. However, this force is in the opposite direction to that due to the gate-induced stress, and it is not clear what the resulting position of the defect atom should be, although it should depend on the local competition of the two opposing forces. Based on the broadened interface trap spectrum after long-term negative gate bias stress (see figure 30(*a*)), it seems that the resulting distribution of the positions of the defect atoms spans a rather wide range, suggesting that the two opposing forces are not spatially uniform over the area of the device.

The similarity between the (110) and (111) results is quite interesting. Since it has been shown theoretically that the local environment of the dangling-bond defect at the (110)Si/SiO_2 interface is very similar to that at the (111)Si/SiO_2 interface [9], which is also consistent with ESR measurements [11], the interpretation given to the (111) results may also be applied to the (110) results.

Unfortunately, for our (100) results we do not yet have any plausible explanation which allows us to properly take into account the effects of the various experimental parameters. This is partly due to the fact that the experimental results are too complicated, and partly due to the lack of adequate theoretical work in the (100) system with sufficient details to be useful as a guide.

So far we have emphasised the differences among the different orientations. There are, however, important similiarities which should not be overlooked. Let us list a few: (i) right after irradiation, samples of all different orientations exhibit a characteristic peak above the midgap; (ii) given sufficient time, all samples exhibit a peak below the midgap at approximately the same energy position; (iii) the peak below the midgap seems to be more stable than the peak above the midgap. These features must also be considered in future theoretical modelling.

One aspect of the aforementioned items (i) and (ii) may be worth pointing out here; that is, while the starting point and the end point appear to be the same for both (100) and (111) samples (peak 1 right after irradiation eventually ends up as peak 2, even for (100) samples at elevated temperatures), the paths are distinctly different. For (111) samples the peak traverses continuously across the Si band gap until its final, energy stable destination; for (100) samples, on the other hand, there seem to be only two preferred energy states: one corresponding to the initial state and one final.

The fact that the final state (peak 2 below the midgap) is more stable than the initial state (the characteristic

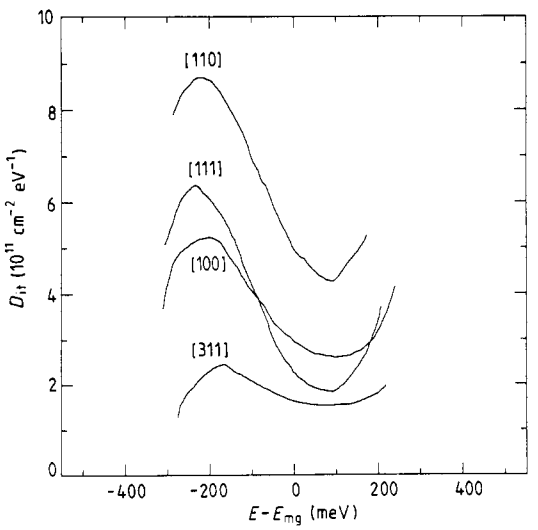

Figure 35. As-grown interface trap distributions of a set of samples with four different Si surface orientations. After dry O_2 oxidation at 1000 °C all samples received post-oxidation-anneal in N_2, but no PMA.

peak above the midgap right after irradiation) is consistent with the observation that a single interface-trap peak below the midgap exists in as-oxidised (100) and (111) samples (with post-oxidation anneal) [10]. Figure 35 shows the as-grown interface trap distribution in a set of samples with four different orientations. These samples were oxidised in dry O_2 at 1000 °C, followed by annealing in N_2 at the growth temperature. No post-metal anneal was given to these samples. They also did not receive any radiation damage. Note that, independent of the orientation, all four samples exhibit a peak below the midgap and its energy position is roughly the same as that of peak 2 discussed throughout this paper. If this peak is indeed the same as peak 2, then this peak is stable at the oxidation temperature, 1000 °C in this case. In the presence of hydrogen, however, this peak can be annealed out at a much lower temperature, and therefore it is not observed after PMA. In our time-dependent studies, annealing of this peak has indeed been observed, which may also be partly due to the presence of hydrogen in the oxide, at the Al/SiO_2 interface, or in the ambient.

Acknowledgments

The author would like to thank Dr Y Nishioka and Dr E F da Silva Jr for the experimental results on (100) samples, and Mr Y Wang for the experimental results on (111) and other orientations. He would also like to acknowledge the help of GE, TI and Hitachi for supplying some of the MOS capacitors used in this work, and NRL for supplying the (111), (110) and (311) wafers. Thank is also due to Drs E Poindexter and A Edwards for suggesting the (111) experiment, and to Dr A Edwards for valuable discussions on the (111) results. This work was supported by a grant from SRC and grant from NRL.

References

[1] Winokur P S, McGarrity J M and Boesh Jr H E 1976 Dependence of interface-state buildup on hole generation and transport in irradiated MOS capacitors *IEEE Trans. Nucl. Sci.* **NS-23** 1580

[2] Winokur P S, Boesh Jr H E, McGarrity J M and McLean F B 1977 Field- and time-dependent radiation effects at the SiO_2/Si interface of hardened MOS capacitors *IEEE Trans. Nucl. Sci.* **NS-24** 2113

[3] Winokur P S, Boesh Jr H E, McGarrity J M and McLean F B 1979 Two-stage process for buildup of radiation-induced interface states *J. Appl. Phys.* **50** 3492

[4] Poindexter E H and Edwards A H Private communications

[5] Edwards A H 1987 Theory of the P_b center at the (111) Si/SiO_2 interface *Phys. Rev.* B **36** 9638

[6] Zekeriya V and Ma T P 1984 Dependence of x-ray generation of interface traps on gate metal induced interfacial stress in MOS structures *IEEE Trans. Nucl. Sci.* **NS-31** 1261

[7] Wang Y, Nishioka Y, Ma T P and Barker R C 1988 Radiation and hot-electron effects on SiO_2/Si interfaces with oxides grown in O_2 containing small amounts of trichloroethane *Appl. Phys. Lett.* **52** 573

[8] Gerardi G J, Poindexter E H, Caplan P J and Johnson N M 1986 Interface traps and P_b centers in oxidized (100) silicon wafers *Appl. Phys. Lett.* **49** 348

[9] Carrico A S, Elliott R J and Barrio R A 1986 Model of electronic states at the $Si-SiO_2$ interface *Phys. Rev.* B **34** 872

[10] Johnson N M, Bartelink D J and McVittie J P 1979 Measurement of interface defect states at oxidized silicon surface by constant-capacitance DLTS *J. Vac. Sci. Technol.* **16** 1407

[11] Poindexter E H and Caplan P J 1983 Characterization of Si/SiO_2 interface defects by electron spin resonance *Prog. Surf. Sci.* **14** 201